



Published in final edited form as:

*Leukemia*. 2019 December ; 33(12): 2805–2816. doi:10.1038/s41375-019-0491-z.

## Imipridone ONC212 activates orphan G protein-coupled receptor GPR132 and integrated stress response in acute myeloid leukemia

Takenobu Nii<sup>1,†</sup>, Varun V. Prabhu<sup>2,†</sup>, Vivian Ruvolo<sup>1</sup>, Neel Madhukar<sup>3</sup>, Ran Zhao<sup>1</sup>, Hong Mu<sup>1</sup>, Lauren Heese<sup>1</sup>, Yuki Nishida<sup>1</sup>, Kensuke Kojima<sup>1,4</sup>, Mathew J. Garnett<sup>5</sup>, Ultan McDermott<sup>5</sup>, Cyril H. Benes<sup>6</sup>, Neil Charter<sup>7</sup>, Sean Deacon<sup>7</sup>, Olivier Elemento<sup>3</sup>, Joshua E. Allen<sup>2</sup>, Wolfgang Oster<sup>2</sup>, Martin Stogniew<sup>2</sup>, Jo Ishizawa<sup>1,\*</sup>, Michael Andreeff<sup>1,\*</sup>

<sup>1</sup>Section of Molecular Hematology and Therapy, Department of Leukemia, The University of Texas MD Anderson Cancer Center, Houston, TX;

<sup>2</sup>Oncocutics, Inc., Philadelphia, PA;

<sup>3</sup>Institute for Computational Biomedicine, Weill Cornell Medicine, New York, NY;

<sup>4</sup>Division of Hematology, Respiratory Medicine and Oncology, Department of Internal Medicine, Saga University, Saga, Japan;

<sup>5</sup>Wellcome Trust Sanger Institute, Wellcome Genome Campus, Cambridge, UK;

<sup>6</sup>Department of Medicine, Massachusetts General Hospital, Boston, MA;

<sup>7</sup>DiscoverX Corporation, Fremont, CA.

### Abstract

Imipridones constitute a novel class of anti-tumor agents. Here, we report that a second-generation imipridone, ONC212, possesses highly increased anti-tumor activity compared to the first-generation compound ONC201. *In vitro* studies using human acute myeloid leukemia (AML) cell lines, primary AML, and normal bone marrow (BM) samples demonstrate that ONC212 exerts prominent apoptogenic effects in AML, but not in normal BM cells, suggesting potential clinical utility. Imipridones putatively engage G protein-coupled receptors (GPCRs) and/or trigger an integrated stress response in hematopoietic tumor cells. Comprehensive GPCR screening identified ONC212 as activator of an orphan GPCR GPR132 and Gαq signaling, which functions

Users may view, print, copy, and download text and data-mine the content in such documents, for the purposes of academic research, subject always to the full Conditions of use:[http://www.nature.com/authors/editorial\\_policies/license.html#terms](http://www.nature.com/authors/editorial_policies/license.html#terms)

\*Co-corresponding authors.

†Both authors contributed equally to this work.

**Corresponding authors:** Michael Andreeff MD, PhD ([mandreeff@mdanderson.org](mailto:mandreeff@mdanderson.org)), Jo Ishizawa, MD, PhD ([Jishizawa@mdanderson.org](mailto:Jishizawa@mdanderson.org)), Section of Molecular Hematology and Therapy, Department of Leukemia, Unit 448, The University of Texas MD Anderson Cancer Center, 1515 Holcombe Boulevard, Houston, TX 77030.

Author contributions:

TN, JI, VVP, KK, JEA, WO, MS and MA conceived and designed the study. TN, JI, VVP, NM, VR, LH, RZ, YN, SD, JEA and HM acquired the data. TN, JI, VVP, YN, NM, KK, MJG, UM, CHB, NC, OE, JEA, MS and MA analyzed and interpreted the data. TN, JI, VVP, KK, JEA, MS, WO and MA wrote, reviewed and/or revised the manuscript.

**Conflict of interest statement:** VVP, JEA, WO, and MS are employees and stockholders of Oncocutics. MA is a member of the scientific advisory board of Oncocutics and stock holder.

as a tumor suppressor. Heterozygous knock-out of GPR132 decreased the anti-leukemic effects of ONC212. ONC212 induced apoptogenic effects through the induction of an integrated stress response, and reduced MCL-1 expression, a known resistance factor for BCL-2 inhibition by ABT-199. Oral administration of ONC212 inhibited AML growth *in vivo* and improved overall survival in xenografted mice. Moreover, ONC212 abrogated the engraftment capacity of patient-derived AML cells in an NSG PDX model, suggesting potential eradication of AML initiating cells, and was highly synergistic in combination with ABT-199. Collectively, our results suggest ONC212 as a novel therapeutic agent for AML.

## Keywords

AML; apoptosis; G protein-coupled receptor; ONC212

---

## Introduction

Acute myeloid leukemia (AML) encompasses a group of highly heterogeneous hematological malignancies, some of which can carry poor prognosis. Standard chemotherapy has not changed over the past 40+ years and acquired resistance leading to disease relapse typically occurs in the majority of AML patients. Better understanding of the disease in the last decade has led to the development of multiple targeted therapeutics that are being investigated in pre-clinical models and clinical trials, and breakthrough discoveries in elderly AML treated with ABT-199 (Bcl-2 inhibition) combination.

Imipridones encompass a new class of anti-tumor small molecules that were created following the discovery of the lead compound ONC201 [1], which is in clinical trials for several advanced malignancies including leukemias, myelomas, lymphomas and gliomas [2, 3]. ONC201 demonstrated an exceptional pharmacokinetic and pharmacodynamic safety profile and encouraging evidence of anti-tumor activity [4]. ONC201 was putatively determined to antagonize the G protein-coupled receptor (GPCR) superfamily dopamine receptors D2 and D3 (DRD2/3) [5], and by us and others to activate an atypical integrated stress response (ISR) [6, 7]. By way of this novel mechanism of action, ONC201 was reported to induce apoptosis in numerous human cancer types that were resistant to standard-of-care therapeutics without causing cytotoxicity in normal cells [7, 8].

The GPCR superfamily is the largest and most diverse group of cell surface receptors in mammals. In a pathophysiological context, GPCRs are involved in cancer initiation, promotion, and metastasis [9], and play pivotal roles in activating major proliferative and survival signal transduction pathways relevant to cancer cells [10, 11]. Thus, GPCRs are considered promising therapeutic targets in cancer [12].

In view of the therapeutic opportunities available within the GPCR superfamily, ONC201's therapeutic index [1, 2, 7], and its novel tri-heterocyclic core chemical structure [13], a series of second-generation analogs were generated [14]. In this study, we report the effects of one such compound, ONC212, on AML, and a novel therapeutic mechanism targeting the orphan GPCR GPR132 and ISR. In addition, we report on unique combinatorial approaches that extend these anti-cancer effects.

## Materials and Methods

### Cell culture

Cell lines were purchased from Leibniz-Institut Deutsche Sammlung von Mikroorganismen und Zellkulturen or the American Type Culture Collection. The authenticity of the cell lines was confirmed by DNA fingerprinting with the short tandem repeat method, using a PowerPlex 16 HS System (Promega, WI, USA) within 6 months before the experiments. All cell lines were tested using the PCR Mycoplasma Detection Kit (Applied Biological Materials, Richmond, BC, Canada) as directed by the manufacturer. The mantle cell lymphoma (MCL) line JeKo-1 was cultured in RPMI 1640 medium containing 20% fetal bovine serum (FBS), AML lines (OCI-AML3, MOLM-13, MOLM-14, MV4;11, KG-1, Kasumi-1, U937, HL-60, and THP-1), T cell leukemia (Jurkat and JurkatI9.2) [15], DDIT3 (CHOP) knockdown cells which we previously established [7] and the colorectal cancer cell line HCT-116 were all cultured in RPMI 1640 medium containing 10% FBS; wild type and Bax and Bak double knock out mouse embryonic fibroblasts (MEFs) were cultured in MEM $\alpha$  1640 medium containing 20% FBS. ONC201-resistant (ONC-R) cell lines were generated by chronic exposure of MCL and AML cell lines to ONC201 whose ED50s for ONC201 at 72 h were all > 5  $\mu$ M, as described previously [7]. To generate HCT-116 GPR132 knock-out cells, we used the PITCh system gene knock-in method previously established [16]. A GFP knock-in cell line at the AAVS1 locus was used as control. Details are described in Supplemental Methods.

### Reagents and Drug treatment

ONC201 and ONC212 were manufactured and provided by Oncocotics Inc., Philadelphia, PA. ABT-199 for the in vitro experiments was purchased from Selleck Chemicals LLC (Houston, TX, USA) and for in vivo experiments from Active Biochemku LTD (Maplewood, NJ, USA). Doxorubicin was purchased from Bedford Laboratories, Bedford, Ohio, USA. For 72-h drug treatment experiments, cell lines were plated at a density of  $1.5 \times 10^5$ /ml for JeKo-1, OCI-AML3, MOLM-13, MOLM-14, MV4;11, KG-1, U937;  $3.0 \times 10^5$ /ml for Kasumi-1, HL-60, THP-1, Jurkat, and JurkatI9.2;  $5.0 \times 10^5$ /ml for HCT-116; and treated with the indicated compounds. For 120-h drug treatment experiments, cell lines were plated at a density of  $5.0 \times 10^4$ /ml for OCI-AML3 and U937 and  $1.0 \times 10^5$ /ml for Kasumi-1, KG-1, HL-60, and THP-1. For ISR activation, 1  $\mu$ M thapsigargin (6 h) were used.

### Flow cytometric analysis

For apoptosis analysis, annexin V (BD Pharmingen, CA, USA) and propidium iodide (PI; Sigma-Aldrich, MO, USA) were used to assess apoptosis. annexin V- and PI-double negative cells were counted as live cells. To determine absolute cell numbers, CountBright beads (Thermo Fisher Scientific, MA, USA) were added to each sample. For cell cycle analysis, DNA content analysis was performed by staining with PI and 5-ethynyl-2'-deoxyuridine (EdU) incorporation was analyzed by Click-iT EdU Alexa Fluor 647 Flow Cytometry Assay Kit (Thermo Fisher Scientific), as per manufacturer's instructions. To measure mitochondrial membrane potential (MMP), we loaded cells with MitoTracker Red CMXRos (300 nM) and MitoTracker Green (100  $\mu$ M, both from Molecular Probes, Eugene, OR, USA) for 1 h at 37°C. The MMP was then assessed by measuring CMXRos retention

(red fluorescence), whereas simultaneously adjusting for mitochondrial mass (green fluorescence) [17].

### Statistical analyses

Differences among groups were analyzed for statistical significance with GraphPad Prism 6 software (Graph-Pad Software, San Diego, CA, USA) using a Student's *t*-test or ANOVA followed by Tukey's post hoc test. A  $p < 0.05$  was considered statistically significant. Unless otherwise indicated, values are expressed as the mean  $\pm$  SD calculated by performing three or more independent experiments. For drug combination analysis, synergistic effects of drugs were analyzed by CompuSyn software, ComboSyn Inc., Paramus, NJ, USA. The combination index (CI) provides quantitative determination for synergism ( $CI < 1$ ), additive effect ( $CI = 1$ ) and antagonism ( $CI > 1$ ) [18, 19].

## Results

### ONC212 exhibits potent anti-tumor effects via the activation of orphan GPCR GPR132

We recently reported that the first generation imipridone ONC201 putatively antagonizes DRD2/3 [5]. Therefore, we speculated that imipridones in general could selectively target the GPCR superfamily of proteins. Experimental GPCR profiling using the PathHunter  $\beta$ -arrestin assay [20] determined that ONC212 (Fig. 1A) was highly selective for activating the orphan GPCR GPR132 (Fig. 1B). Although six hits were identified from the initial screen with this single high concentration of ONC212, multi-dose validation studies confirmed that ONC212 only engaged GPR132 at nanomolar concentrations ( $EC_{50} \sim 400$  nM) (Fig. 1C and Table S3). We further performed the bioSensAll assays to determine which  $G\alpha$  isoform was engaged downstream of GPR132, and demonstrated that  $G\alpha_q$  family proteins ( $G\alpha_q$ ,  $G\alpha_{14}$ , and  $G\alpha_{15/16}$ ) are specifically activated via GPR132 by ONC212 (Fig. 1D and Fig. S1) while  $G\alpha_s$  family proteins were not (Fig. S1). The activation of  $G\alpha_q$  was blocked by the  $G\alpha_q$  inhibitor UBO (Fig. 1D), indicating the specificity of detected bioluminescence resonance energy transfer (BRET) signals. Interestingly,  $G\alpha_q$  activation varied with pH, consistent with GPR132 being a pH sensitive GPCR [21] (Fig. S2).

To further assess the impacts of GPR132 on cytotoxic effects of ONC212 in tumor cells, we generated HCT-116 GPR132 knock-out cells by gene knock-in method using CRISPR/Cas9 [16] (Fig. S3A). We identified one heterozygous knock-out clone, which has a knock-in allele and in-frame 27 base-pair deletion on the other allele (Fig. 1E and Fig. S3B). The GPR132 heterozygous knock-out decreased ONC212's apoptogenic effects (Figs. 1F and 1G), further supporting a role for GPR132 in this process. Interestingly, GPR132 knock-down by shRNA decreased target levels by approximately 50%, but ONC212 increased GPR132 levels above baseline; hence this system could not be used to determine impact of GPR132 on activity (data not shown).

RNA-seq data available in The Cancer Genome Atlas (TCGA) revealed that GPR132 is expressed in a wide range of tumor types, with highest expression in leukemias and lymphomas (<http://www.cbioportal.org/>) without any reported loss-of-function gene mutations (Fig. S4). Previous studies have implicated GPR132 as tumor suppressor [22, 23],

suggesting that activation of GPR132 by ONC212 could exert growth inhibitory and apoptotic effects. We analyzed the *in vitro* anti-tumor effects of ONC212 in the GDSC collection of cell lines (i.e., 1,088 human cancer cell lines) and found that leukemias and lymphomas were most sensitive (Fig. S5A). When we further analyzed types of leukemias, AML, acute lymphoblastic leukemia (ALL), and chronic myeloid leukemia (CML) lines were all similarly sensitive to ONC212 (Fig. S5B and S5E). In support of the therapeutic relevance of GPR132 for ONC212 anti-tumor activity, expression of GPR132 mRNA was positively correlated with sensitivity to ONC212 (Fig. 1H), based on gene expression profiling data in the GDSC panel. Moreover, we compared GPR132 expression between human primary AML and normal hematopoietic samples in the RNA-seq data from TCGA and The Genotype-Tissue Expression (GTEx) projects using Gene Expression Profiling Interactive Analysis (GEPIA) [24]. The AML patient samples significantly higher levels of GPR132 expression compared to normal samples (Fig. 1I). Since a threshold level for normal hematopoietic cells has not been established, the lack of observed toxicity could be related to lower levels of GRP132. These data suggest that GPR132 could be a potential therapeutic target, particularly in AML.

### ONC212 induces apoptosis in AML cells

We assessed ONC212's efficacy and mechanisms in AML cells. We first tested the apoptogenic effects of ONC212 in a series of AML cell lines (Figs. 2A and 2B). Compared with the ED50s of ONC201 that we reported previously [7], ONC212 exerted markedly enhanced apoptogenic effects [ED50s of ONC201 [7] vs ONC212 (Fig. 2A) at 72 h; 6.4  $\mu$ M vs 258.7 nM for OCI-AML3, 3.6  $\mu$ M vs 105.7 nM for MOLM13 cells, respectively], indicating that this agent was > 30-fold more potent than the parent compound.

Several cell lines were relatively insensitive 72 h after ONC212 exposure (Fig. 2A), but became apoptotic at 120 h (Fig. 2B and Fig. S6A). Time course analysis of OCI-AML3 cells showed that induction of apoptosis took more than 36 h and gradually increased in a time-dependent manner (Figs. 2C and 2D). ONC212 reduced mitochondrial membrane potential (MMP), suggesting mitochondrial apoptosis (Fig S7A and S7B), consistent with previously reported GPR132-mediated mitochondrial apoptosis [25]. In addition, Bax and Bak double knock-out MEFs showed resistance to ONC212, compared to wild-type MEFs (Figs. S7C and S7D). Of note, ONC201-resistant (ONC-R) cell lines [7] showed cross-resistance to ONC212 (Figs. 2E and 2F, Fig. S6A-S6D), suggesting common resistance mechanisms for the two compounds. Also, as reported for ONC201 [7], ONC212 increased  $\gamma$ H2A.X only to the extent seen in Nutlin-3a treated cell, which was selected as a compound that induces only minimal DNA damage [26] (Fig. S6E). This finding suggests that ONC212 is non-genotoxic, which is a potential advantage for its clinical implementation.

We also performed wash-out experiments of ONC212 to investigate how long this agent is required to be present to induce irreversible apoptosis. Unlike ONC201, which at least a 72 hr exposure is required for apoptosis induction, only 12 hr of exposure to ONC212 was sufficient (Figs. 2G and 2H).

GPR132 mRNA expression was detected in all tested AML cell lines (Fig. S8A). There was a statistically significant correlation between the level of apoptosis induction by ONC212

and GPR132 mRNA expression in the AML cell lines tested (Fig. S8B). However, THP-1 and Kasumi-1 cells, which respond only slowly and display the lowest sensitivity to ONC212, were outliers (Fig. 2B) [7]. In addition, ONC212 treatment transcriptionally increased GPR132 expression (Fig. S8C), suggesting that the apoptogenic effects of ONC212 reflect not only functional activation of GPR132, but also on its transcriptional induction.

### **ONC212 efficiently induces cell death in patient-derived AML, but not normal hematopoietic cells**

Next, we examined the effects of ONC212 on human primary AML and normal BM cells (Fig. S9A). ONC212 treatment inhibited blast colony formation in a dose-dependent manner (Fig. 3A and 3B and Fig. S9B). Importantly, in normal BM cells there were no marked effects by ONC212 on colony formation (Fig. 3C) and differentiation potential of hematopoietic progenitor cells (Fig. 3D and Fig. S9C). ONC212 also did not affect cell viability of normal BM and lung fibroblasts at doses that were efficacious in this regard in malignant cells (Fig. S10). These results suggested that ONC212 exerts selective toxicity in leukemia as compared to non-malignant cells.

### **ONC212 dysregulates cell cycle progression resulting in anti-proliferative effects in AML cells**

To examine the cell cycle effects of ONC212, we analyzed the incorporation of EdU and DNA content in AML cell lines. ONC212 treatment increased the percentage of G0/G1 and decreased S- and G2/M cells and EdU incorporation in S phase in MOLM13 and HL-60 cells (Figs. S11A-S11E). In particular, ONC212 treatment induced a more prominent G0/G1 arrest in MOLM13 than in HL-60 cells (Fig. S11A). To confirm the growth inhibitory effects of ONC212, we counted the number of viable cells at early time points before apoptosis was induced and indeed, the proliferation of viable cells was inhibited by ONC212 (Figs. S11F and S11G) at 24 h indicating a cytostatic effect on AML cells.

### **ONC212 exhibits anti-leukemia activity *in vivo***

For assessing ONC212's anti-leukemia effects on leukemia-initiating cells (LICs), we utilized an established PDX mouse model [7]. Bulk AML cells [t(9;11)(p22; q23), CEBPA and ATM mutants] from secondarily engrafted mice (i.e., LIC-enriched PDX cells) were incubated *ex vivo* for 36 h with or without 250 nM of ONC212. We then injected identical numbers of viable treated and untreated cells into recipient NSG mice. After one month, the percentage of human CD45<sup>+</sup> cells in the peripheral blood (PB), spleen, and BM was significantly decreased in the ONC212-treated group compared to the untreated control (Fig. 4A and Fig. S12A). Spleens collected from the treated mice were significantly smaller than those obtained from the controls (Figs. S12B and S12C). These results suggested that ONC212 impairs the engraftment capacity of LICs.

We next administered ONC212 orally to mice bearing two different AML xenografts. In the first model, MV4;11 cells were subcutaneously injected into the right and left flank of mice. Mice were treated with cytarabine, ONC201, or ONC212 when the tumors reached a detectable volume. ONC212 significantly reduced leukemia xenograft growth as well as the

cytarabine treatment, while ONC201 was not efficacious in this model at similar doses (Fig. 4B). Of note, more frequent dosing with lower doses of ONC212 (5 or 25 mg/kg) did not inhibit leukemia progression (Fig. 4B and Fig. S13).

As second model, we utilized systemic AML xenografts. OCI-AML3 cells expressing luciferase were injected into NSG-S mice via tail vein and monitored by bioluminescence imaging (BLI). After confirmation of AML engraftment after 7 d (Fig. 4C), mice were treated with oral administration of ONC212, serial BLI images showed that ONC212 significantly inhibited AML growth as soon as during the wk of therapy (Figs. 4C). Moreover, ONC212 treatment decreased spleen leukemia burden (Fig. 4D) and prolonged overall survival compared with controls ( $p = 0.0003$ ; Fig. 4E). The median survival increased from 43 to 49 d (+14%). Consistently, AML cell infiltration in BM and spleens of the ONC212-treated mice was reduced, as indicated by spleen size (Fig. 4D) and flow cytometric analysis (Fig. S14). These results indicated that ONC212 exerts anti-leukemia activity *in vivo*. The most effective dose/schedule remains to be established.

### **ONC212 activates an ISR in AML cells and synergized with the BCL-2 inhibitor ABT-199 *in vitro* and *in vivo***

We and others previously reported that an ISR-like pathway involving ATF4 was one of the major molecular mechanisms involved in apoptosis induced by ONC201 in solid and hematologic tumors [6, 7], and comparable induction of ISR by ONC212 was recently also reported in pancreatic cancer cells [27]. Similarly, 24 and 36 h treatment with ONC212 increased phospho-eIF2 $\alpha$  and ATF4 protein abundance (Fig. 5A). *DDIT3* (*CHOP*) mRNA, a transcriptional target of ATF4, and its target genes *GADD34*, *DR5*, and *TRIB3* were also upregulated in ONC212-treated AML cells by a 24-h exposure to ONC212 (Fig. 5B).

To investigate the potential link of the ISR pathway with GPR132-G $\alpha$  q signaling, we analyzed key effector molecules of ISR in the heterozygous GPR132 knock-out HCT-116 cells. *DDIT3* (*CHOP*) induction appeared lower, while resultant induction of the *CHOP* downstream genes (*DR5* and *GADD34*) was observed at a similar level compared to those in control HCT-116 cells (Fig. S15A). This suggests that CHOP signaling is perhaps independent of GPR132-G $\alpha$  q signaling activated by ONC212. Next, to investigate the involvement of ISR in ONC212-induced apoptosis, we tested the role of DR5 and CHOP the two major molecules which could function as an apoptogenic effectors. We first tested the DR5-related extrinsic apoptosis pathway by using Jurkat I9.2 cells carrying inactivated mutant caspase 8 [15]. The mutant Jurkat cells were only slightly less sensitive than parental Jurkat cells, showing 60 to 80% apoptosis at nanomolar concentrations of ONC212 (Fig. S15B), suggesting that DR5 and its downstream apoptotic signaling are only minimally involved in ONC212-induced apoptosis. We also tested CHOP knock down (KD) OCI-AML3 cells that we previously established [7]. The CHOP KD cells were more sensitive to ONC212 than control cells (Fig. S15C and S15D), indicating that CHOP plays an anti-apoptotic role in ONC212-induced apoptosis, a result similar to our previous finding with ONC201 [7]. More comprehensive screening of ISR-related molecules would be required to determine which ISR effectors contribute most to ONC212-induced apoptosis. Of note, in ONC212-resistant (ONC-R) OCI-AML3 cells, an increase of ATF4 by ONC212 was not

observed (Fig. S15E). There was no change in baseline GPR132 expression levels between parental versus ONC-R cells (Fig. S8A). Therefore, the observed resistance in OCI-AML3 ONC-R cells occurs perhaps upstream of ISR induction, but is not caused by reduction in basal expression levels of GPR132.

ONC201 was reported to transcriptionally induce TRAIL in solid tumors [1], but this mechanism was found by us not to be operational in hematological malignancies [7]. Similarly, ONC212 did not increase TRAIL mRNA in OCI-AML3 cells, and rather decreased it in MOLM13 and HL-60 cells (Fig. S15F).

BCL-2 has been implicated as a protective factor in cells under ISR [7, 28–33]. Also importantly, ONC212 markedly reduced MCL-1 protein levels (Fig. S16), is the key resistance factor for BCL-2 inhibition in AML [34]. Consequently, apoptosis induction was significantly increased by combined treatment with ONC212 and the BCL-2 inhibitor ABT-199 compared to either drug alone, even in THP-1 cells, which were the most resistant cells to both ONC212 and ABT-199, as well as in ONC-R OCI-AML3 cells (Fig. 5C-5F and Figs. S17 and S18), suggesting that this combination could potentially overcome resistance to either agent alone.

We further investigated combinatorial regimen *in vivo* using a systemic AML model employing MOLM13-Luc cells intravenously injected into NSG-S mice. After confirmation of AML engraftment (3 d after injection), the mice were treated orally with ABT-199 and/or ONC212. Serial BLI analysis showed that ONC212 in combination with ABT-199 inhibited AML progression (Fig. 6A), resulting in highly significant prolongation of survival compared to the effects exerted by either drug alone (Fig. 6B and 6C). Median survival increased from 20 to 21 d (+5% for ONC212 and ABT-199, respectively) to 30 d, a 50% percent increase for the combination,  $p < 0.0001$ ). Of note, this AML model of MOLM13 is highly aggressive with only approximately 20-d median survival, which may have reduced the potential survival benefit of the monotherapy groups of ONC212 or ABT-199, compared to the OCI-AML3 model shown in Figure 4E. This also implicates that the combination therapy is able to exert a prominent anti-AML effects in such an aggressive type of AML model, where single treatments with ABT-199 or ONC212 was completely ineffective.

## Discussion

In this study, we investigated a novel, second-generation imipridone ONC212, which is a derivative of ONC201. ONC201 is now in multiple clinical trials for leukemias, lymphomas, myelomas, and solid tumors. We show that ONC212 activates the orphan GPCR GPR132, a novel target in hematological malignancies. ONC212 exerts anti-tumor activities in a broad range of cancers and our detailed studies in AML demonstrate that ONC212 potently induces apoptosis in AML cell lines expressing high levels of GPR132, with significant *in vivo* efficacy. These anti-AML effects were much more potent than those observed for ONC201 and as potent as those reported by us and others for the BCL-2 inhibitor ABT-199 (venetoclax). Collectively, we propose a novel therapeutic strategy by activating GPR132, using the novel GPR132 activator ONC212.

The functions of GPR132 in cancer biology are poorly understood, but Lin et al. demonstrated that forced expression of GPR132 results in mitochondrial apoptosis [25]. Activation of GPR132 was shown to inhibit BCR-ABL-induced acute B-cell lymphoblastic leukemia [23]. We here demonstrate that ONC212 directly and transcriptionally activates GPR132, efficiently induces apoptosis in AML cells that highly express GPR132. Moreover, heterozygous knock-out of GPR132 decreases the apoptogenicity of ONC212. Given these results, this orphan GPCR represents a potential therapeutic target for cancer therapy.

The link between GPR132 and ISR induced by ONC212 is unclear. Considering that GPR132 heterozygous KO in HCT-116 did not reduce ATF4-CHOP signaling by ONC212, we speculate that these two pathways are independent. However, since ISR were not induced by ONC212 in OCI-AML3 ONC-R cells which are highly resistant to ONC212-induced (namely, GPR132-mediated) apoptosis, we also speculate activation of a common upstream target for ISR and GPR132 activation. A better mechanistic understanding of how GPR132-Gaq signaling induces apoptosis has yet to be developed in future studies.

ONC212 induced the apoptosis as we reported for ONC201 [7]. Moreover, by targeting BCL-2, a pro-survival factor against apoptosis [28, 30–33], the combination treatment of ONC212 and ABT199 was found highly synergistic, as validated in our AML xenograft model. ABT-199 and related BCL-2 inhibitors currently in clinical trials have shown anti-leukemia activity as monotherapy [35] and pronounced synergy with standard chemotherapy and demethylating agents [36]. This synergism could be also explained by our finding that ONC212 reduces protein abundance of MCL-1, which is known to be the most important resistance factor for ABT-199 in AML [34]. Therefore, ONC212 and ABT-199 are efficiently targeting each other's resistance factors. Considering the low response rate to therapy with ABT-199 and high relapse rate even after ABT199 and azacitidine or Cytarabine [37–39], the concept of combining ONC212 with BH3 mimetics, including Bcl-2 and Mcl-1 inhibitors, could provide excellent rationale for highly effective and non-genotoxic novel drug combinations in AML. This concept is supported by the strategy combining Bcl-2 and Mcl-1 targeted agents [40–42], or Bcl-2 and MDM2 inhibition [43] in pre-clinical survival extension similar to the ones shown here for the combination of ONC212 and ABT-199 [43], which is presently validated in a clinical trial [44] with 50% CR in relapsed/refractory AML the proposed combinatorial treatment appears promising.

Taken together, selectively targeting GPR132 by imipridone ONC212 maybe a promising therapeutic strategy for AML. The present study provides the first reported evidence of therapeutically targeting GPR132 in oncology. Based on our preclinical findings, further development of ONC212 is in progress to enable the clinical evaluation of this novel agent in patients with advanced hematologic malignancies.

## Supplementary Material

Refer to Web version on PubMed Central for supplementary material.

## Acknowledgments

This work was supported in part by grants from National Institutes of Health (P01CA055164), Cancer Prevention Research Institute of Texas (CPRIT, RP121010), the Paul and Mary Haas Chair in Genetics (to MA), the MD Anderson's Cancer Center Support Grant (CA016672) (to MA); the Japan Heart Foundation/Bayer Yakuhin Research Grant Abroad and International Research Fund for Subsidy of Kyushu University School of Medicine Alumni (to TN); NIH Leukemia SPORE Career Enhancement Programs (to JI); and Oncoceutics, Inc. GDSC screening was supported by a grant from the Wellcome Trust (102696).

## References

- Allen JE, Krigsfeld G, Mayes PA, Patel L, Dicker DT, Patel AS, Dolloff NG, Messaris E, Scata KA, Wang W, Zhou JY, Wu GS, El-Deiry WS. Dual inactivation of Akt and ERK by TIC10 signals Foxo3a nuclear translocation, TRAIL gene induction, and potent antitumor effects. *Sci Transl Med.* 2013; 5: 171ra17. doi: 10.1126/scitranslmed.3004828.
- Allen JE, Kline CLB, Prabhu VV, Wagner J, Ishizawa J, Madhukar N, Lev A, Baumeister M, Zhou L, Lulla A, Stogniew M, Schalop L, Benes C, et al. Discovery and clinical introduction of first-in-class imipridone ONC201. *Oncotarget.* 2016; 7: 74380–92. doi: 10.18632/oncotarget.11814. [PubMed: 27602582]
- Arrillaga-Romany I, Chi AS, Allen JE, Oster W, Wen PY, Batchelor TT. A phase 2 study of the first imipridone ONC201, a selective DRD2 antagonist for oncology, administered every three weeks in recurrent glioblastoma. *Oncotarget.* 2017; 8(45): 79298–304. doi: 10.18632/oncotarget.17837. [PubMed: 29108308]
- Stein MN, Bertino JR, Kaufman HL, Mayer T, Moss R, Silk A, Chan N, Malhotra J, Rodriguez L, Aisner J, Aiken RD, Haffty BG, DiPaola RS, et al. First-in-Human Clinical Trial of Oral ONC201 in Patients with Refractory Solid Tumors. *Clin Cancer Res.* 2017; 23: 4163–9. doi: 10.1158/1078-0432.ccr-16-2658. [PubMed: 28331050]
- Kline CLB, Ralff MD, Lulla AR, Wagner JM, Abbosh PH, Dicker DT, Allen JE, El-Deiry WS. Role of Dopamine Receptors in the Anticancer Activity of ONC201. *Neoplasia.* 2018; 20: 80–91. doi: 10.1016/j.neo.2017.10.002. [PubMed: 29216597]
- Kline CL, Van den Heuvel AP, Allen JE, Prabhu VV, Dicker DT, El-Deiry WS. ONC201 kills solid tumor cells by triggering an integrated stress response dependent on ATF4 activation by specific eIF2alpha kinases. *Sci Signal.* 2016; 9: ra18. doi: 10.1126/scisignal.aac4374. [PubMed: 26884600]
- Ishizawa J, Kojima K, Chachad D, Ruvolo P, Ruvolo V, Jacamo RO, Borthakur G, Mu H, Zeng Z, Tabe Y, Allen JE, Wang Z, Ma W, et al. ATF4 induction through an atypical integrated stress response to ONC201 triggers p53-independent apoptosis in hematological malignancies. *Sci Signal.* 2016; 9: ra17. doi: 10.1126/scisignal.aac4380. [PubMed: 26884599]
- Allen JE, Crowder R, El-Deiry WS. First-In-Class Small Molecule ONC201 Induces DR5 and Cell Death in Tumor but Not Normal Cells to Provide a Wide Therapeutic Index as an Anti-Cancer Agent. *PLoS One.* 2015; 10: e0143082. doi: 10.1371/journal.pone.0143082. [PubMed: 26580220]
- Dorsam RT, Gutkind JS. G-protein-coupled receptors and cancer. *Nat Rev Cancer.* 2007; 7: 79–94. doi: 10.1038/nrc2069. [PubMed: 17251915]
- Lynch JR, Wang JY. G Protein-Coupled Receptor Signaling in Stem Cells and Cancer. *Int J Mol Sci.* 2016; 17. doi: 10.3390/ijms17050707.
- Lappano R, Maggiolini M. G protein-coupled receptors: novel targets for drug discovery in cancer. *Nat Rev Drug Discov.* 2011; 10: 47–60. doi: 10.1038/nrd3320. [PubMed: 21193867]
- Jones LH, Bunnage ME. Applications of chemogenomic library screening in drug discovery. *Nat Rev Drug Discov.* 2017; 16(4): 285–96. doi: 10.1038/nrd.2016.244. [PubMed: 28104905]
- Wagner J, Kline CL, Pottorf RS, Nallaganchu BR, Olson GL, Dicker DT, Allen JE, El-Deiry WS. The angular structure of ONC201, a TRAIL pathway-inducing compound, determines its potent anti-cancer activity. *Oncotarget.* 2014; 5: 12728–37. doi: 10.18632/oncotarget.2890. [PubMed: 25587031]
- Wagner J, Kline CL, Ralff MD, Lev A, Lulla A, Zhou L, Olson GL, Nallaganchu BR, Benes CH, Allen JE, Prabhu VV, Stogniew M, Oster W, et al. Preclinical evaluation of the imipridone family, analogues of clinical stage anti-cancer small molecule ONC201, reveals potent anti-cancer effects

- of ONC212. *Cell Cycle*. 2017; 16(19): 1790–9. doi: 10.1080/15384101.2017.1325046. [PubMed: 28489985]
15. Juo P, Woo MSA, Kuo CJ, Signorelli P, Biemann HP, Hannun YA, Blenis J. FADD is required for multiple signaling events downstream of the receptor Fas. *Cell Growth and Differentiation*. 1999; 10: 797–804. doi: [PubMed: 10616904]
  16. Sakuma T, Nakade S, Sakane Y, Suzuki KT, Yamamoto T. MMEJ-assisted gene knock-in using TALENs and CRISPR-Cas9 with the PITCh systems. *Nat Protoc*. 2016; 11: 118–33. doi: 10.1038/nprot.2015.140. [PubMed: 26678082]
  17. Kojima K, Konopleva M, Tsao T, Andreeff M, Ishida H, Shiotsu Y, Jin L, Tabe Y, Nakakuma H. Selective FLT3 inhibitor FI-700 neutralizes Mcl-1 and enhances p53-mediated apoptosis in AML cells with activating mutations of FLT3 through Mcl-1/Noxa axis. *Leukemia*. 2010; 24: 33–43. doi: 10.1038/leu.2009.212. [PubMed: 19946262]
  18. Chou TC, Motzer RJ, Tong Y, Bosl GJ. Computerized quantitation of synergism and antagonism of taxol, topotecan, and cisplatin against human teratocarcinoma cell growth: a rational approach to clinical protocol design. *J Natl Cancer Inst*. 1994; 86: 1517–24. doi: [PubMed: 7932806]
  19. Chou TC. Preclinical versus clinical drug combination studies. *Leuk Lymphoma*. 2008; 49: 2059–80. doi: 10.1080/10428190802353591. [PubMed: 19021049]
  20. Southern C, Cook JM, Neetoo-Isseljee Z, Taylor DL, Kettleborough CA, Merritt A, Bassoni DL, Raab WJ, Quinn E, Wehrman TS, Davenport AP, Brown AJ, Green A, et al. Screening beta-arrestin recruitment for the identification of natural ligands for orphan G-protein-coupled receptors. *J Biomol Screen*. 2013; 18: 599–609. doi: 10.1177/1087057113475480. [PubMed: 23396314]
  21. Justus CR, Dong L, Yang LV. Acidic tumor microenvironment and pH-sensing G protein-coupled receptors. *Front Physiol*. 2013; 4: 354. doi: 10.3389/fphys.2013.00354. [PubMed: 24367336]
  22. Weng Z, Fluckiger AC, Nisitani S, Wahl MI, Le LQ, Hunter CA, Fernald AA, Le Beau MM, Witte ON. A DNA damage and stress inducible G protein-coupled receptor blocks cells in G2/M. *Proceedings of the National Academy of Sciences of the United States of America*. 1998; 95: 12334–9. doi: 10.1073/pnas.95.21.12334. [PubMed: 9770487]
  23. Le LQ, Kabarowski JH, Wong S, Nguyen K, Gambhir SS, Witte ON. Positron emission tomography imaging analysis of G2A as a negative modifier of lymphoid leukemogenesis initiated by the BCR-ABL oncogene. *Cancer Cell*. 2002; 1: 381–91. doi: [PubMed: 12086852]
  24. Tang Z, Li C, Kang B, Gao G, Li C, Zhang Z. GEPIA: a web server for cancer and normal gene expression profiling and interactive analyses. *Nucleic acids research*. 2017; 45: W98–W102. doi: 10.1093/nar/gkx247. [PubMed: 28407145]
  25. Lin P, Ye RD. The lysophospholipid receptor G2A activates a specific combination of G proteins and promotes apoptosis. *J Biol Chem*. 2003; 278: 14379–86. doi: 10.1074/jbc.M209101200. [PubMed: 12586833]
  26. Verma R, Rigatti MJ, Belinsky GS, Godman CA, Giardina C. DNA damage response to the Mdm2 inhibitor nutlin-3. *Biochem Pharmacol*. 2010; 79: 565–74. doi: 10.1016/j.bcp.2009.09.020. [PubMed: 19788889]
  27. Lev A, Lulla AR, Wagner J, Ralff MD, Kiehl JB, Zhou Y, Benes CH, Prabhu VV, Oster W, Astsaturov I, Dicker DT, El-Deiry WS. Anti-pancreatic cancer activity of ONC212 involves the unfolded protein response (UPR) and is reduced by IGF1-R and GRP78/BIP. *Oncotarget*. 2017; 8: 81776–93. doi: 10.18632/oncotarget.20819. [PubMed: 29137221]
  28. Akl H, Vervloessem T, Kiviluoto S, Bittremieux M, Parys JB, De Smedt H, Bultynck G. A dual role for the anti-apoptotic Bcl-2 protein in cancer: mitochondria versus endoplasmic reticulum. *Biochim Biophys Acta*. 2014; 1843: 2240–52. doi: 10.1016/j.bbamcr.2014.04.017. [PubMed: 24768714]
  29. Cheng EH, Wei MC, Weiler S, Flavell RA, Mak TW, Lindsten T, Korsmeyer SJ. BCL-2, BCL-X(L) sequester BH3 domain-only molecules preventing BAX- and BAK-mediated mitochondrial apoptosis. *Mol Cell*. 2001; 8: 705–11. doi: [PubMed: 11583631]
  30. Sano R, Reed JC. ER stress-induced cell death mechanisms. *Biochim Biophys Acta*. 2013; 1833: 3460–70. doi: 10.1016/j.bbamcr.2013.06.028. [PubMed: 23850759]

31. Kornblau SM, Thall PF, Estrov Z, Walterscheid M, Patel S, Theriault A, Keating MJ, Kantarjian H, Estey E, Andreeff M. The prognostic impact of BCL2 protein expression in acute myelogenous leukemia varies with cytogenetics. *Clin Cancer Res.* 1999; 5: 1758–66. doi: [PubMed: 10430080]
32. Ishizawa J, Kojima K, McQueen T, Ruvolo V, Chachad D, Noguera-Gonzalez GM, Huang X, Pierceall WE, Dettman EJ, Cardone MH, Shacham S, Konopleva M, Andreeff M. Mitochondrial Profiling of Acute Myeloid Leukemia in the Assessment of Response to Apoptosis Modulating Drugs. *PLoS One.* 2015; 10: e0138377. doi: 10.1371/journal.pone.0138377. [PubMed: 26375587]
33. Cory S, Adams JM. The BCL2 family: Regulators of the cellular life-or-death switch. *Nature Reviews Cancer.* 2002; 2: 647–56. doi: 10.1038/nrc883. [PubMed: 12209154]
34. Pan R, Hogdal LJ, Benito JM, Bucci D, Han L, Borthakur G, Cortes J, DeAngelo DJ, Debose L, Mu H, Dohner H, Gaidzik VI, Galinsky I, et al. Selective BCL-2 inhibition by ABT-199 causes on-target cell death in acute myeloid leukemia. *Cancer Discov.* 2014; 4: 362–75. doi: 10.1158/2159-8290.cd-13-0609. [PubMed: 24346116]
35. Konopleva M, Pollyea DA, Potluri J, Chyla B, Hogdal L, Busman T, McKeegan E, Salem AH, Zhu M, Ricker JL, Blum W, DiNardo CD, Kadia T, et al. Efficacy and Biological Correlates of Response in a Phase II Study of Venetoclax Monotherapy in Patients with Acute Myelogenous Leukemia. *Cancer Discov.* 2016; 6: 1106–17. doi: 10.1158/2159-8290.cd-16-0313. [PubMed: 27520294]
36. DiNardo C, Pollyea D, Pratz K, Thirman MJ, Letai A, Frattini M, Jonas B, Levenson J, Zhu M, Dunbar M. A phase 1b study of venetoclax (ABT-199/GDC-0199) in combination with decitabine or azacitidine in treatment-naïve patients with acute myelogenous leukemia who are to 65 years and not eligible for standard induction therapy. *Blood.* 2015; 126: 327-. doi:
37. Pollyea DA, Stevens BM, Jones CL, Winters A, Pei S, Minhajuddin M, D'Alessandro A, Culp-Hill R, Riemondy KA, Gillen AE, Hesselberth JR, Abbott D, Schatz D, et al. Venetoclax with azacitidine disrupts energy metabolism and targets leukemia stem cells in patients with acute myeloid leukemia. *Nature Medicine.* 2018; 24: 1859–66. doi: 10.1038/s41591-018-0233-1.
38. Pollyea DA, Jordan CT. Why are hypomethylating agents or low-dose cytarabine and venetoclax so effective? *Curr Opin Hematol.* 2019; 26: 71–6. doi: 10.1097/moh.0000000000000485. [PubMed: 30652974]
39. Nakada D Venetolax with Azacitidine Drains Fuel from AML Stem Cells. *Cell Stem Cell.* 2019; 24: 7–8. doi: 10.1016/j.stem.2018.12.005. [PubMed: 30609400]
40. Grundy M, Balakrishnan S, Fox M, Seedhouse CH, Russell NH. Genetic biomarkers predict response to dual BCL-2 and MCL-1 targeting in acute myeloid leukaemia cells. *Oncotarget.* 2018; 9: 37777–89. doi: 10.18632/oncotarget.26540. [PubMed: 30701031]
41. Bate-Eya LT, den Hartog IJ, van der Ploeg I, Schild L, Koster J, Santo EE, Westerhout EM, Versteeg R, Caron HN, Molenaar JJ, Dolman ME. High efficacy of the BCL-2 inhibitor ABT199 (venetoclax) in BCL-2 high-expressing neuroblastoma cell lines and xenografts and rational for combination with MCL-1 inhibition. *Oncotarget.* 2016; 7: 27946–58. doi: 10.18632/oncotarget.8547. [PubMed: 27056887]
42. Liu T, Wan Y, Liu R, Ma L, Li M, Fang H. Design, synthesis and preliminary biological evaluation of indole-3-carboxylic acid-based skeleton of Bcl-2/Mcl-1 dual inhibitors. *Bioorg Med Chem.* 2017; 25: 1939–48. doi: 10.1016/j.bmc.2017.02.014. [PubMed: 28233676]
43. Pan R, Ruvolo V, Mu H, Levenson JD, Nichols G, Reed JC, Konopleva M, Andreeff M. Synthetic Lethality of Combined Bcl-2 Inhibition and p53 Activation in AML: Mechanisms and Superior Antileukemic Efficacy. *Cancer Cell.* 2017; 32: 748–60.e6. doi: 10.1016/j.ccell.2017.11.003. [PubMed: 29232553]
44. Daver N, Pollyea DA, Yee KWL, Fenau P, Brandwein JM, Vey N, Martinelli G, Kelly KR, Roboz GJ, Garcia JS, Pigneux A, Kshirsagar S, Dail M, et al. Preliminary Results from a Phase Ib Study Evaluating BCL-2 Inhibitor Venetoclax in Combination with MEK Inhibitor Cobimetinib or MDM2 Inhibitor Idasanutlin in Patients with Relapsed or Refractory (R/R) AML. *Blood.* 2017; 130: 813-. doi:

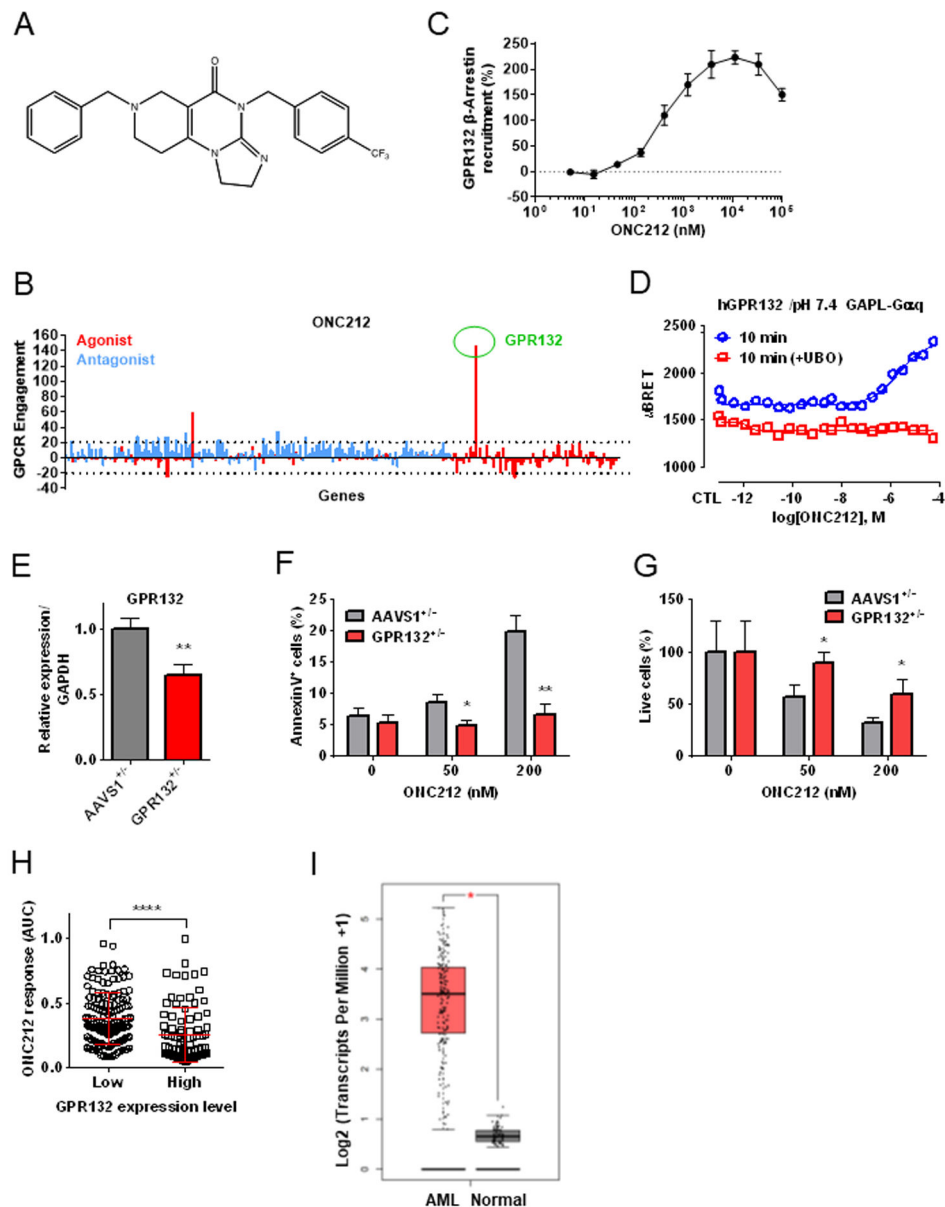


**Figure 1. Target screening of G protein-coupled receptors (GPCRs) identifies GPR132 as a receptor of ONC212.**

(A) Chemical structure of ONC212. (B) ONC212 (10  $\mu$ M) target screening in GPCRs performed with PathHunter  $\beta$ -Arrestin assay. Dotted line indicates a 20% cut-off to select targets for subsequent validation. (C) ONC212 dose-response curve in the PathHunter  $\beta$ -Arrestin assay for GPR132. EC<sub>50</sub> = 405 nM (n = 2). (D) Cells were pre-treated for 1h with UBO-QIC (100 nM). Experimental data were produced in singleton and curves were fitted using the 4-parameter logistic non-linear regression model (GraphPad 6). Data in graphs represent a 10 min incubation with ONC212 and expressed as uBRET. (E) qRT-PCR analysis of GPR132 expression. GFP heterozygous knock-in at GPR132 locus (GPR132<sup>+/-</sup>; GPR132 heterozygous knock-out) and at AAVS1 locus (AAVS1<sup>+/-</sup>; gene knock-in control). (F) The percentage of apoptotic cells (AnnexinV<sup>+</sup> cells) induced by ONC212 treatment for

72 h in GPR132<sup>+/-</sup> and AAVS1<sup>+/-</sup>. (G) The percentage of live cell numbers after 72 h-treatment with ONC212 in GPR132<sup>+/-</sup> and AAVS1<sup>+/-</sup>. (H) Average ONC212 response as measured by the area under the dose-response curve (AUC) in GDSC cell lines with high versus low GPR132 expression. \*\*\*\*; P < 0.001. (I) comparison of GPR132 expression in AML and normal samples using Gene expression profiling interactive analysis (GEPIA). AML (n=173) and Normal (n=70) \*; p < 0.01,

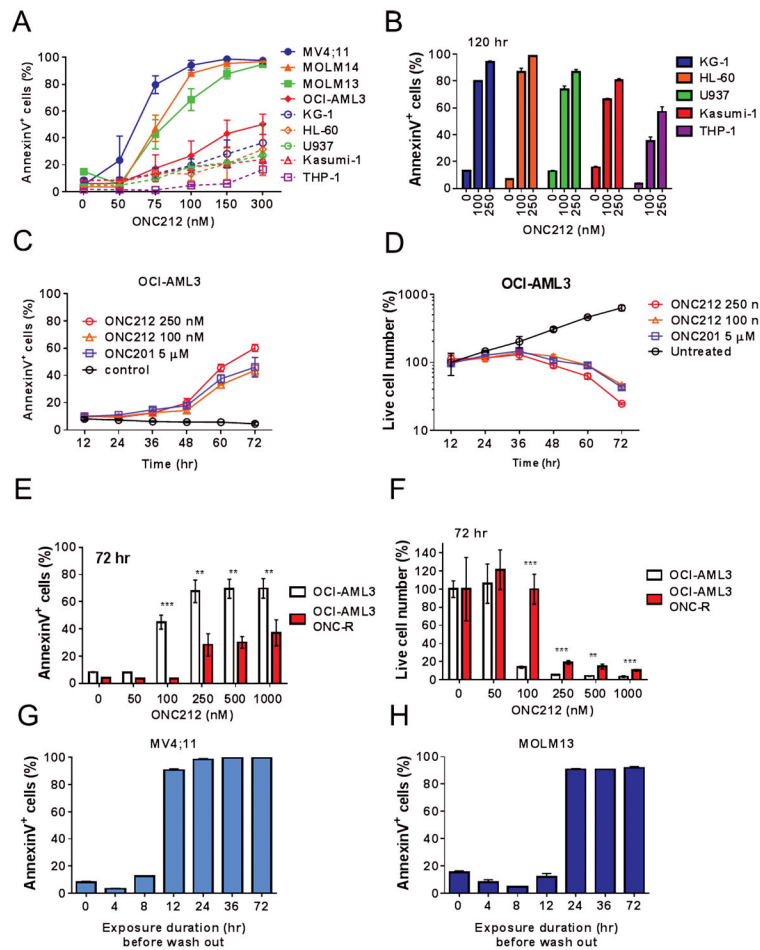


**Figure 2. Assessment of ONC212 potency in AML cells.**

(A) Summary data of ONC212's effects on several AML cell lines at the indicated concentration for 72 h. (B) The percentage of apoptotic cells induced by ONC212 treatment for 120 h in KG-1, HL-60, U937, Kasumi-1, and THP-1 cell lines. (C) Time course analysis of apoptosis induced by ONC212 or ONC201 in OCI-AML3 cells. (D) Time course analysis of the percentage of live cells following treatment with ONC212 or ONC201. Annexin V- and PI-negative cells were counted as live cells. (E) The percentage of apoptotic cells induced by ONC212 treatment for 72 h in parental or ONC201-resistant (ONC-R) OCI-AML3 cells. (F) The percentage of live cell numbers after 72 h-treatment with ONC212 in parental or ONC-R OCI-AML3 cells. The percentage of AnnexinV<sup>+</sup> cells of MV4;11 (G) and MOLM13 (H) cells treated with ONC212 (250 nM) for 4, 8, 24, 36, and 72 h. ONC212 medium was replaced by fresh medium at these time points and cell viability was determined at 72 h for all samples. Data are shown as the mean  $\pm$  SD (n = 3). \*\*, p < 0.01, \*\*\*, p < 0.005.

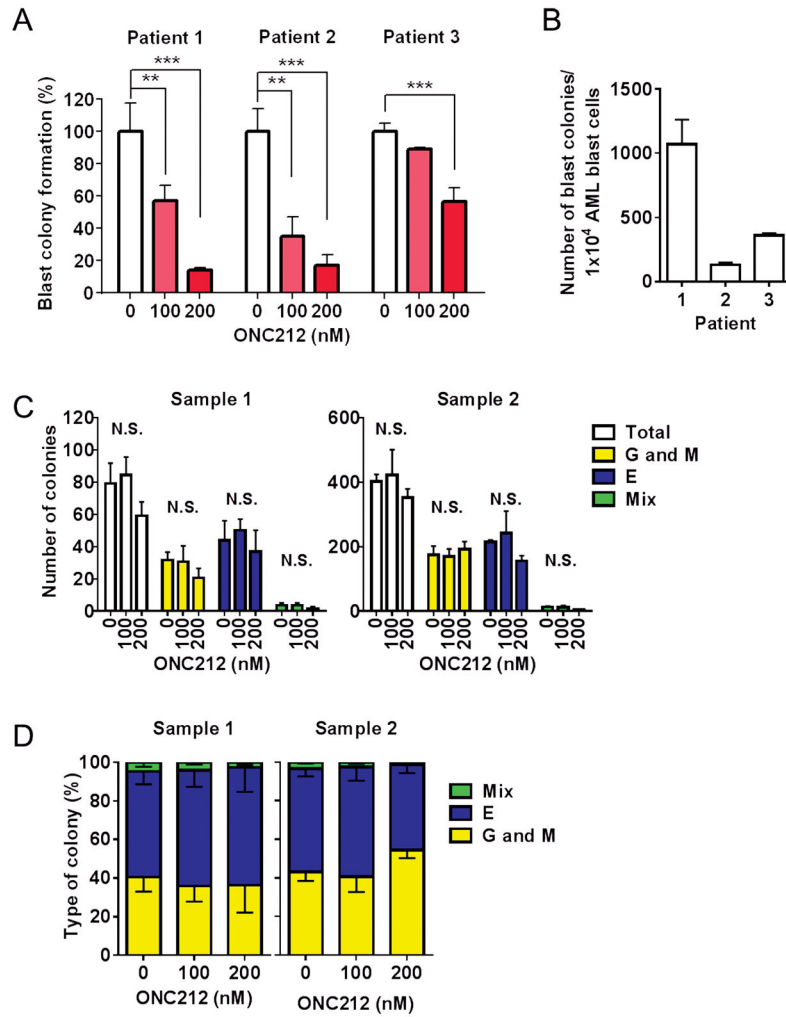


**Figure 3. ONC212 treatment inhibits the clonogenic growth of human AML blasts but not normal hematopoietic cells.**

For treatment with or without ONC212 (100 or 200 nM), (A) the percentage of blast colony formation from three patient samples were examined. \*\*,  $p < 0.01$ , \*\*\*,  $p < 0.005$ . (B) The number of blast colonies from AML patients without ONC212 treatment. (C) Hematopoietic colony formation from two healthy donor BM samples following the above-mentioned treatment. (D) Mean of each type of hematopoietic colony generated in percentage. ONC212 did not affect the frequency of each colonies. Data are shown as the mean  $\pm$  SD ( $n = 3$ ). N.S. = not significant.

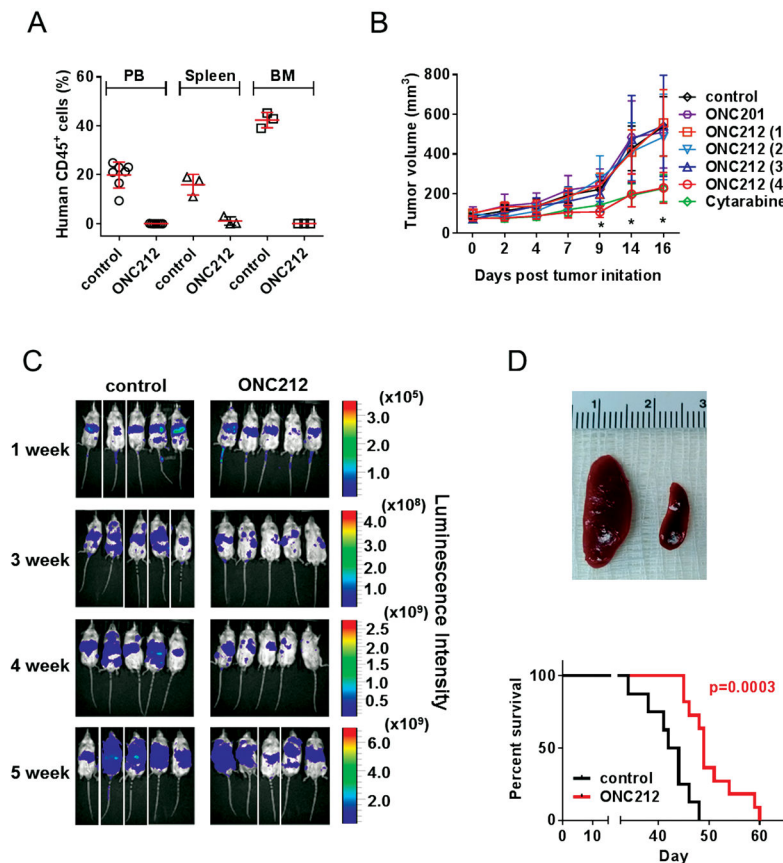


**Figure 4. ONC212 treatment inhibits the leukemia stem and progenitor cells.**

(A, B) *Ex vivo* treatment of primary AML patient-derived xenograft (pdx) cells with ONC212. One month post-injection of pdx-AML cells with or without ONC212 (250 nM), we analyzed human CD45<sup>+</sup> cells in peripheral blood (PB), spleen, and BM. (A) Quantification data of human CD45<sup>+</sup> cells. Data are shown as the mean  $\pm$  SD (n = 3). (B) MV4;11 cells were subcutaneously implanted in the flanks of athymic nude. Tumor volume of AML xenograft model treated with ONC201 (50 mg/kg/wk), ONC212 [(1) 5 mg/kg/wk; (2) 5 mg/kg, twice/wk; (3) 25 mg/kg, twice/wk; (4) 50 mg/kg/wk] and cytarabine (100 mg/kg, 5 times/wk). n=10, \*, p < 0.05 relative to vehicle control. (D-E) NSG-S mice injected OCI-AML3-Luc were treated with or without ONC212 (treatment started on d 7, 50 mg/kg/mice, twice/wk for 7 wk). (C) Serial bioluminescence intensity of mice bearing OCI-AML3-Luc treated with the vehicle or ONC212. ONC212 treatment decreased OCI-AML3 propagation. (D) Picture of spleen from mice injected OCI-AML3-Luc with or without ONC212 treatment after 45 d of OCI-AML3-Luc cells injection. (E) Kaplan-Meier survival curves for mice (control: n = 8, ONC212: n = 11).

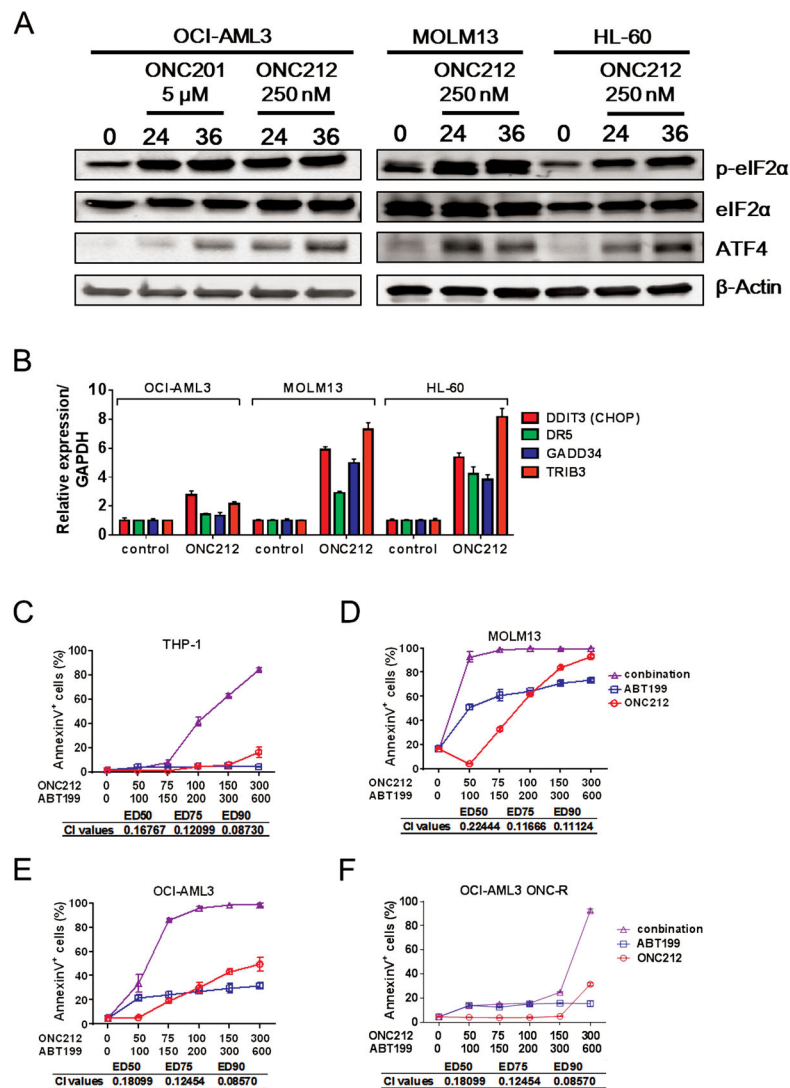


**Figure 5. ONC212 induces integrated stress response and shows synergistic effects with ABT-199.** (A) Western blotting analysis of eIF2 $\alpha$  phosphorylation level and ATF4 expression. We treated OCI-AML3, MOLM13 and HL-60 with or without ONC212 (250 nM) or ONC201 (5  $\mu$ M) for the indicated time. (B) Relative expression level of DDIT3 (CHOP), DR5, GADD34 and TRIB3. We treated OCI-AML3, MOLM13 and HL-60 with or without ONC212 (250 nM) for 24 h and analysis of gene expression by qRT-PCR. The range given for these genes relative to control were determined by evaluating the expression:  $2^{-\Delta\Delta CT}$  with  $CT + s$  and  $CT - s$ , where  $s$  = the SD of the  $CT$  value. (C-F) The percentage of annexin V<sup>+</sup> cells induced by ONC212 and/or ABT-199. All data are shown as the mean  $\pm$  SD ( $n = 3$ ). The combination index (CI) values for synergistic effects were all performed with Compusyn software.

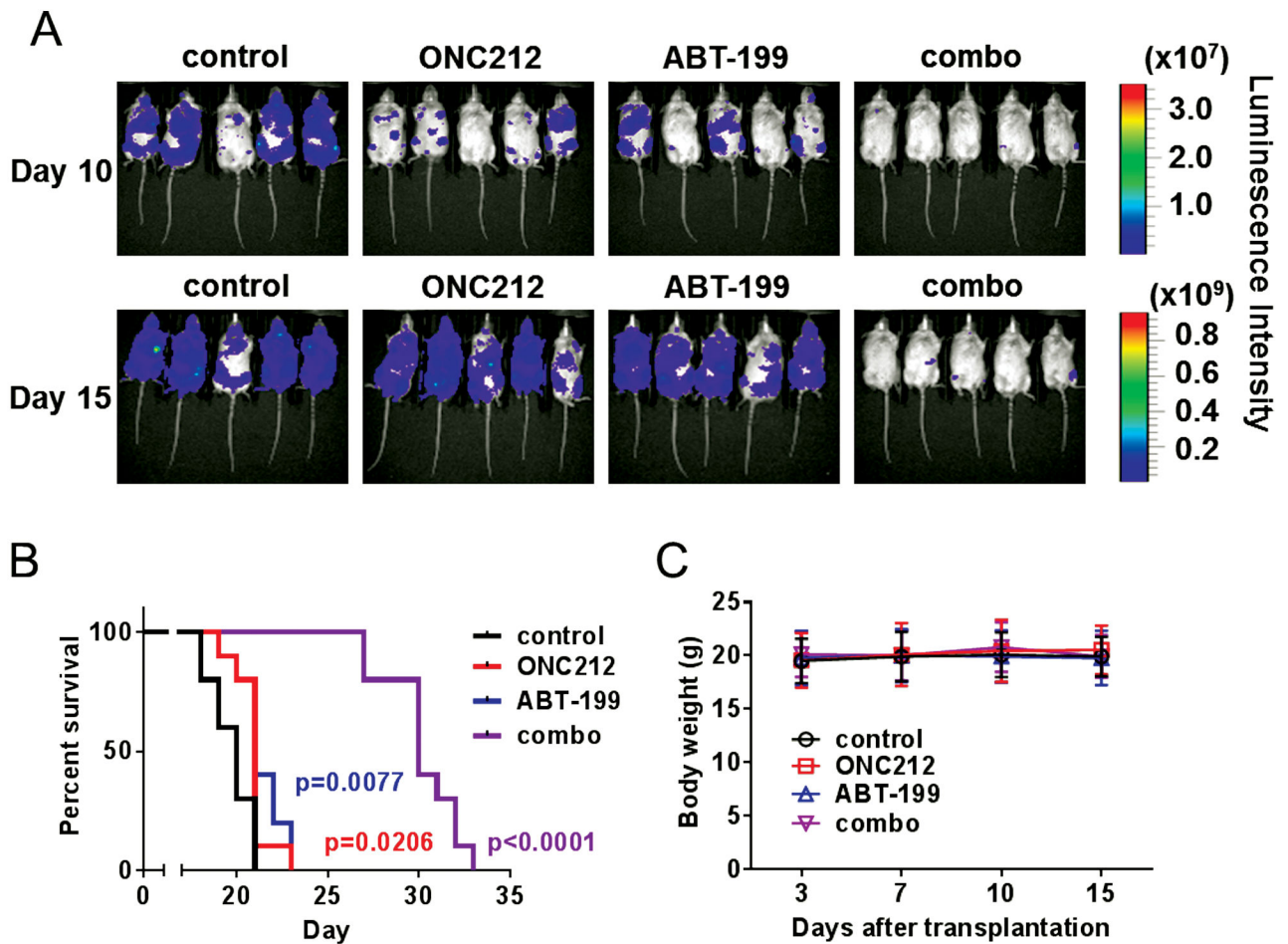


**Figure 6. ONC212 and ABT-199 combination treatment synergistically decreases AML propagation *in vivo*.**

(A) Serial bioluminescence images of mice bearing MOLM13-Luc treated with the solvent, ONC212 (50 mg/kg; 3 times/wk), ABT-199 (100 mg/kg; daily) and combination treatment (treatment started on d three administered by oral gavage). (B) Kaplan–Meier survival curves for mice as described above (n = 10). The survival of the mice was remarkably prolonged by ONC212 and ABT-199 oral gavage treatment. (C) Body weight of mice bearing MOLM13-Luc treated with the solvent, ONC212, ABT-199 and combination treatment (n = 10).